JOURNAL OF SOLID STATE CHEMISTRY 96, 132–140 (1992)

Ba_2PrPtO_6: A Novel Double Perovskite

U. AMADOR, C. J. D. HETHERINGTON, E. MORAN, AND M. A. ALARIO-FRANCO*

Departamento de Química Inorgánica, Facultad de Químicas, Universidad Complutense de Madrid, 28040-Madrid, Spain

Received July 18, 1991

The structure of the Ba_2PrPtO_6 compound has been determined by X-ray powder diffraction and profile analysis and has been confirmed by TEM and HREM. The structure of this material is made up of alternating [PtO_6] and [PrO_6] octahedra along the three *a*, *b*, and *c* directions. Magnetic properties are also presented and discussed. © 1992 Academic Press, Inc.

Introduction

The perovskite structure is one of the most studied among the oxide structures (*1–3*). The aristotype, $SrTiO_3$, is cubic, but many different versions showing lower symmetry are well known (*4–6*). In this connection, there are several cases—for example, $SrSnO_3$—where a double cubic perovskite cell has been suggested to exist (*7*), but a more detailed study (*8*) showed a cell of lower symmetry and the presence of multiple twinning, which gives rise to the fictitious "double" cell. In the case of solids with composition of the type $A_2BB'O_6$ or, in general, in a multiple occupation of the *A* or *B* sublattices, one can understand the doubling of the perovskite cell through an ordering of the cations. Two interesting examples have been reported: La_2LiFeO_6, in which an environment of six weak Li–O bonds enhances the covalency of the Fe–O bonds thereby stabilizing the oxidation state of iron V (*9*), and Pb_2ScTaO_6, which shows both ordered and disordered domains with a size up to 1000 Å (*10*).

In the title compound the doubling of the cell can be achieved by ordering of Pt and Pr ions along the three main directions. This compound is obtained as a by-product in single crystal growth experiments of the Ybacuo family material $Ba_2PrCu_3O_7$ (*11*) due to the reaction of the flux with platinum crucibles. It is worth noting that in single crystal growth experiments of $Ba_2YCu_3O_y$, the formation of the double perovskite $Ba_8Pt_4Y_3O_{17.5}$ has been reported (*12*).

In this paper, a structural study of Ba_2PtPrO_6 by X-ray powder diffraction and profile analysis, and TEM and HREM, is presented together with measurements of its magnetic properties.

Experimental

The sample was synthesized by solid-state reaction at 1253 K from a mixture of Pr_6O_{11}, $BaCO_3$, and PtO_2-nH_2O in the stoichiometric ratio. The platinum oxide was obtained by dissolving platinum powder

* To whom correspondence should be addressed.

0022-4596/92 $3.00

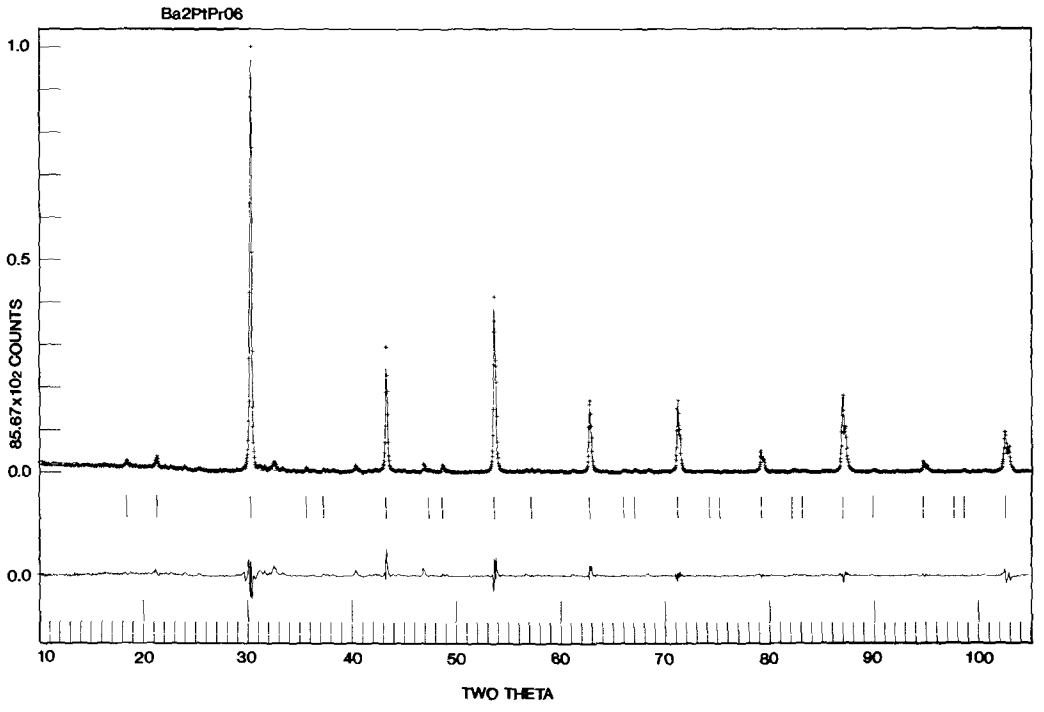

FIG. 1. Experimental and calculated X-ray diffraction patterns for Ba_2PtPrO_6.

with a mixture of nitric and hydrochloric acids, and then precipitating with a Na_2CO_3 solution in water. The value of "n" determined by TGA technique was about 7. This "fresh" platinum oxide seems to be much more reactive than the commercial one.

Powder X-ray diffraction patterns were collected on a Siemens D-500 apparatus in the angular range 10°–105° (2θ) in steps of 0.05°. The structure was refined by the Rietveld method (*13*) using a version of the DBW 3.2 Whiles and Young program (*14*). The peak shape function used was the pseudo-Voigt, with asymmetry correction for 2θ angles below 50°. In the final step of the refinement, all structural and profile parameters were refined simultaneously. The refinement was terminated when the shifts for all parameters were less than 0.3σ.

Electron diffraction and chemical analysis, and high resolution electron microscopy, were performed using a JEOL-2000FX (equipped with an EDS microanalyzer) and a JEOL-4000EX microscope, respectively.

Molar magnetic measurements down to 5 K were performed using an ASMI magnetometer (minimum magnetic field 14 KG and $HdH/dz = 29$ KG^2/cm).

Results and Discussion

The experimental and calculated X-ray diffraction patterns corresponding to the sample are shown in Fig. 1. Although the general aspect of these patterns resembles that of a perovskite, some small peaks cannot be indexed with the $a = 4.19$ Å parameter. Doubling of the three unit cell axes, i.e., keeping the cubic symmetry, allows the indexing of all the peaks with the exception of two very weak peaks which can be attrib-

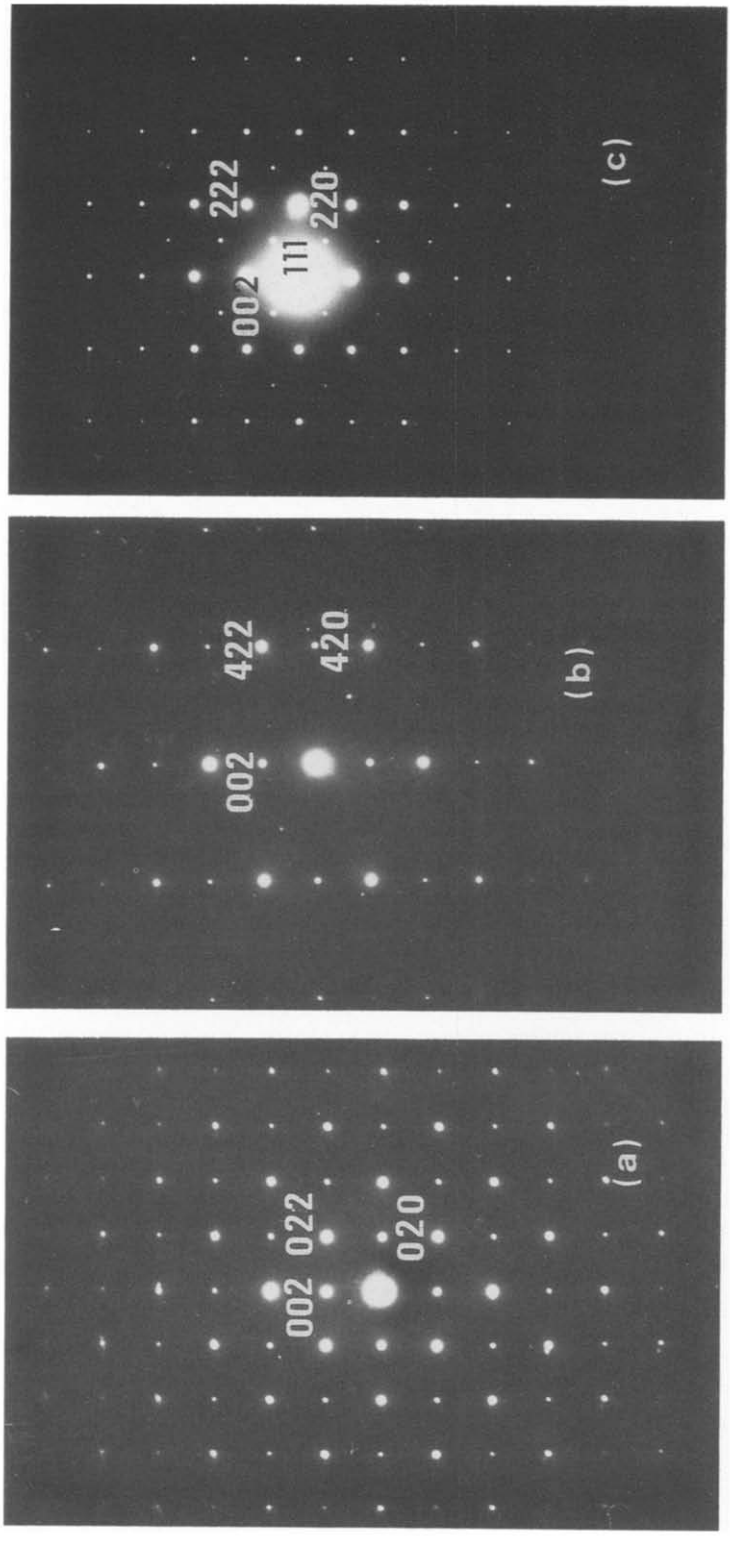

FIG. 2. Electron diffraction patterns taken along: *a*, $[\bar{1}00]$; *b*, $[\bar{1}20]$; *c*, $[\bar{1}10]$. In (c), the (111) spot as indexed in the double cell, or (1/2 1/2 1/2) in the simple one, confirms the doubling of the single cell.

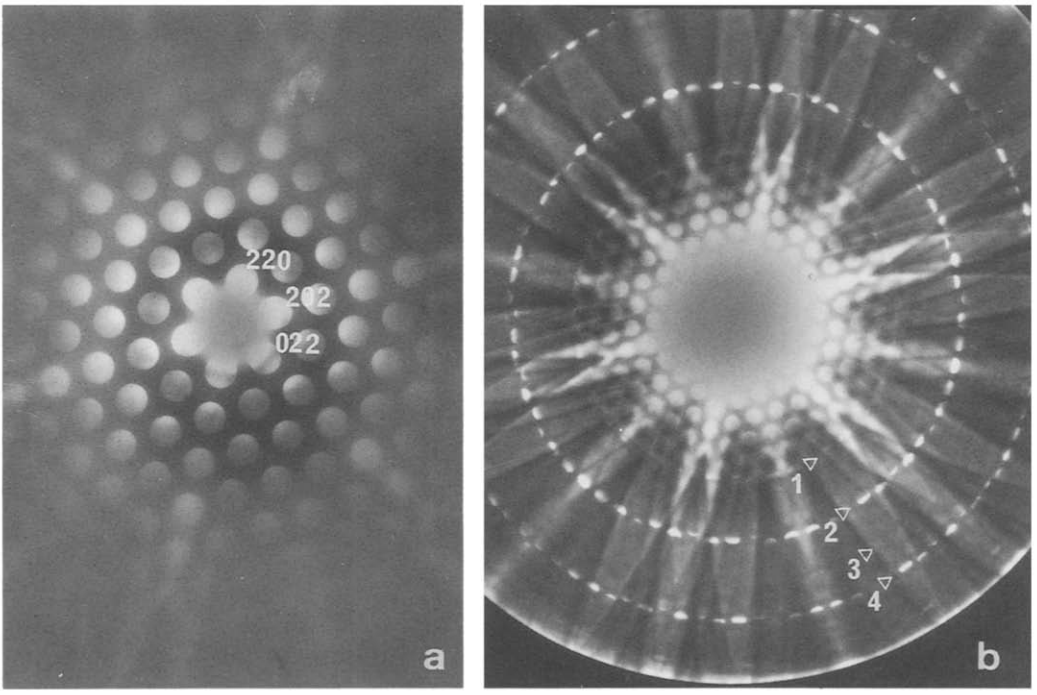

FIG. 3. Convergent beam electron diffraction pattern taken along the $[\bar{1}11]^*$ zone axis: (a), zero order Laue zone; (b), whole pattern showing Laue zones 1–4.

uted to a small amount of impurity. In order to confirm the doubling of the unit cell and determine the symmetry, electron diffraction experiments were performed.

The composition of the material was checked by X-ray energy dispersive microanalysis using the same grains on which the electron diffraction experiments were performed. The presence of barium, praseodymium, and platinum was confirmed.

Figure 2 shows three diagrams corresponding to the following zone axes (double cell indices): *2a*, $[\bar{1}00]$; *2b*, $[\bar{1}20]$; *2c*, $[\bar{1}10]$. Although the first two could be indexed in the smaller cell, the $[\bar{1}10]$ pattern requires the doubling. The (111) spot in the electron diffraction pattern taken along $[\bar{1}10]$ cannot appear by addition of three perpendicular cells of lower symmetry (e.g., tetragonal), or by multiple scattering. Besides, the systematic absences suggest an *F*-type cell. Other reciprocal lattice sections confirmed this assignment.

In order to confirm that doubling of the periodicity occurs along all three cubic axes and that cubic symmetry is retained, convergent beam electron diffraction patterns were taken along the $[\bar{1}11]^*$ axis with a probe size of around 2000 Å at room temperature (Fig. 3). The whole pattern symmetry is $3m$, which confirms that cubic symmetry is not broken. The {220} discs are labeled in Fig. 3(a), as are the HOLZ rings (1, 2, 3, 4) corresponding to levels at multiples of 0.0689 $Å^{-1}$ ($= 1/3\ g_{111}$) in Fig. 3(b). The first and third ring intensities are weak because they are composed of 111-type reflections whose structure factors are small and because of thermal vibrations, but their presence also confirms the ordering of Pt and Pr in the ⟨111⟩ directions.

The ordering of Pt and Pr can be imaged at

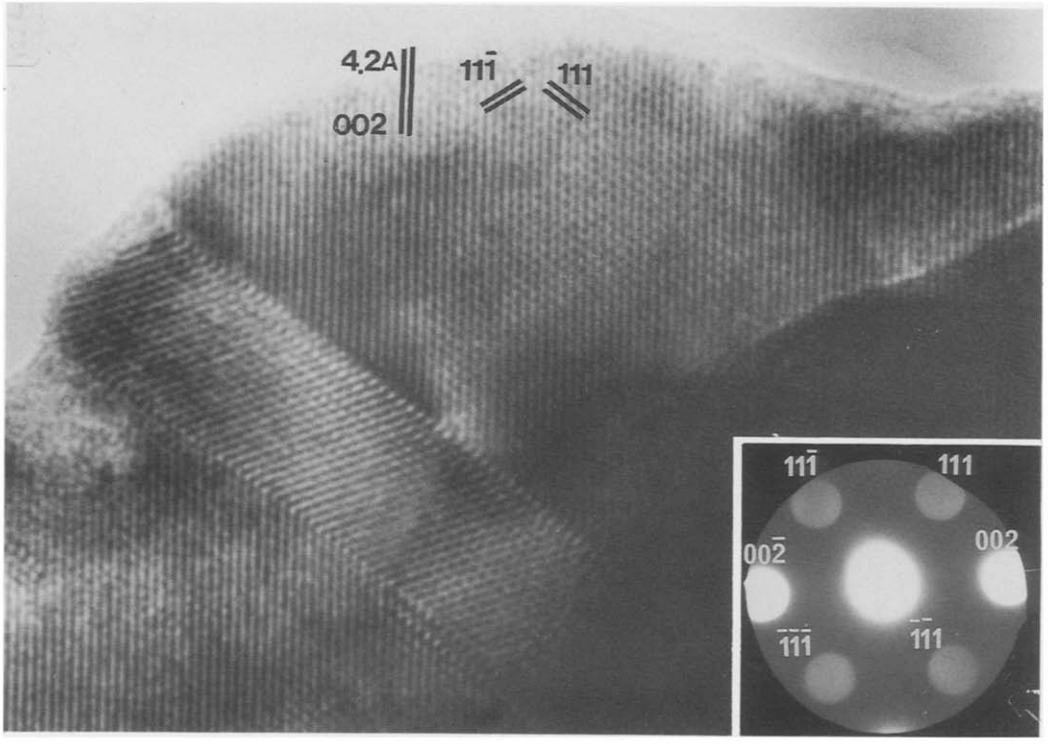

FIG. 4. High resolution superlattice image along [$\bar{1}$10], and (inset), electron diffraction taken from area outside twin band and showing objective aperture of radius 0.27 Å^{-1}.

high resolution along the zone [$\bar{1}$10], which contains two sets of {111} planes end-on. Figure 4 shows an image taken using an objective aperture of radius 0.27 Å^{-1} (resolution 3.7 Å) that excludes the strong 220 and 004 beams. The visibility of the {111} planes is thus enhanced. The inset diffraction pattern was taken from the upper central portion of the image. A twin band is observed in the image: extensive twinning on {111} was present in the sample and will be reported in further detail elsewhere (*15*). The 002 fringes (4.2 Å) are predominant in the image, but the presence of 111 fringes in some regions of the image indicates that ordering is present. The absence of 111 fringes in other regions may be due to disordering brought about during specimen preparation (grinding by mortar and pestel in ethanol) or exposure to the electron beam, or it may indicate that the material is not uniformly ordered. No antiphase domains can be seen, and the ordering is retained in the twinned material.

Other $\bar{1}$10 images were taken at a higher resolution using a larger objective aperture and an example is shown in Fig. 5. The effective aperture radius, which was due to the contrast transfer function, was around 0.55 Å^{-1} (while a real aperture of radius 0.8 Å^{-1} was used to remove some of the non-image-forming electrons.) The image is taken at just under Scherzer defocus so that individual cation columns in the thinnest region of the specimen are resolved as white dots. The appearance of the 2.1 Å-spaced 004 fringes in the 001 direction alternates correspondingly to the composition of the 004 planes that are alternately Ba ions and Pt and Pr ions. Reliable identification requires

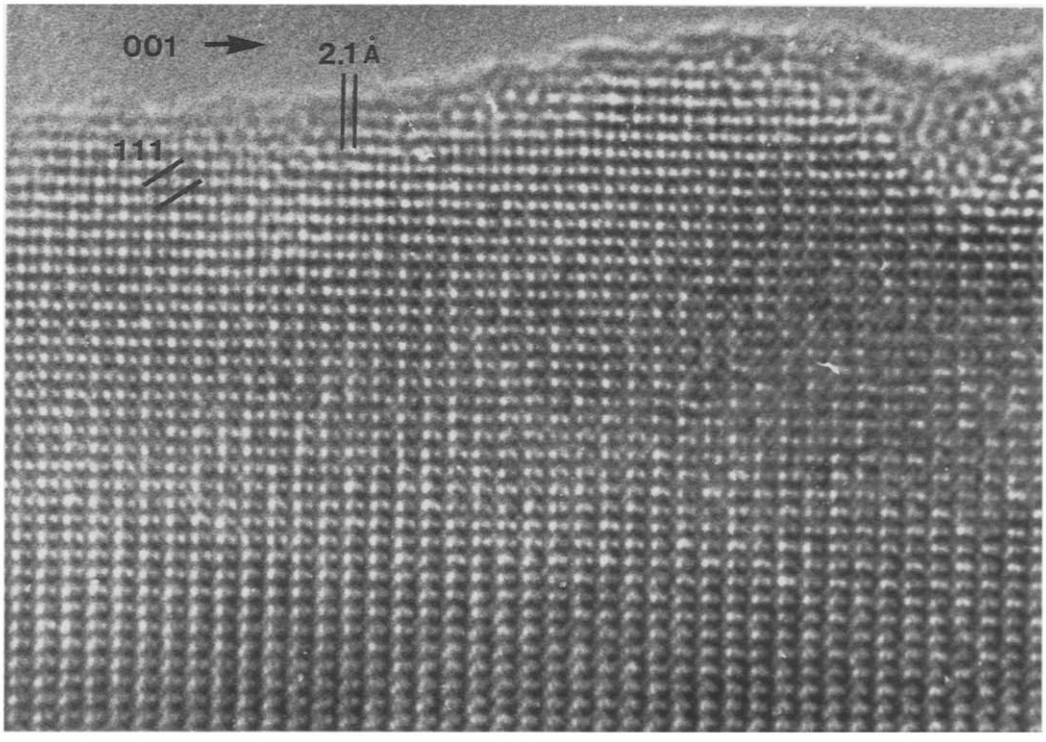

FIG. 5. High resolution image taken along [$\bar{1}$10] showing 004 planes (spacing 2.1 Å) that are alternately Ba and (Pt + Pr). Ordering of Pt and Pr ions in the 111 direction is faintly visible when the image is viewed at an oblique angle.

a comparison with an image simulation (or suitable image processing) and will be reported elswhere (*15*).

However, at this resolution, the Pr/Pt ordering in the structure—the subject of this paper—is not immediately visible. In the ordered structure, the cation columns that lie along each Pt + Pr 004 plane are composed alternately of Pt atoms and of Pr atoms so that, in principle, the intensity of the dots that lie along the 004 fringes should vary accordingly. However, the difference in the projected potential of the Pt and the Pr columns (atomic numbers 78 and 59, respectively) is small relative to the difference in projected potential between the atom columns and tunnels. Hence, in the image shown in Fig. 5, we presume any variation in intensity of the dots due to ordering of the Pt and Pr columns is lost within the image noise. Processing of the image by averaging over several unit cells should reduce the noise sufficiently to reveal the ordering (at the simplest level, this can be achieved by viewing the image from an oblique angle along the 111 planes).

On the basis of the double cell, a refinement of the X-ray powder pattern using the Rietveld method was attempted in the $Fm\bar{3}m$ space group (obtained simply by doubling the perovskite cell and keeping all the symmetry elements).

The structural parameters so obtained are those shown in Table I. The structure is built up by [PrO_6] octahedra and the slightly smaller [PtO_6] octahedra, alternating along the main directions (Fig. 6).

On the other hand, Ba ions are sur-

TABLE I

STRUCTURAL PARAMETERS FOR Ba_2PtPrO_6

Atom	Site	x	y	z	occ
Ba	8*c*	0.25	0.25	0.25	0.12500
Pt	4*a*	0.0	0.0	0.0	0.06250
Pr	4*b*	0.5	0.5	0.5	0.06250
O	24*e*	0.244(4)	0.0	0.0	0.25000

Note. a = 8.3892(2) Å, S.G.: $Fm\bar{3}m$, R_p = 13.4, R_B = 7.7, R_F = 8.4, Z = 4, R_{exp} = 8.9, R_{wp} = 17.7, χ^2 = 3.96.

rounded by 12 oxygen atoms, in a regular arrangement.

According to the structural refinement, an ordering between praseodymium and platinum is established.

From the bond lengths in Table II and using the Brown and Altermatt method (*16*), we have estimated the oxidation state of ions to be: $V_{Ba} \simeq 1.9$, $V_{Pt} \simeq 3.8$, $V_{Pr} \simeq 3.9$. In this connection, in the related material $Ba_8Pt_4Y_3O_{17.5}$ (*12*) the presence of both octahedrally coordinated tetravalent platinum and square-planar coordinated divalent platinum ions has been reported. However, in the title compound, every Pt ion is surrounded by six [PrO_6] octahedra; so, the presence of Pr(IV) forces an octahedral coordination of platinum and a higher oxidation state.

In order to confirm the oxidation state of praseodymium, molar magnetic susceptibility measurements were performed. Figure 7 shows the reciprocal molar magnetic susceptibility as a function of temperature. A Curie–Weiss behavior is observed. A magnetic moment of 2.4(1) MB is obtained, in good agreement with the expected value for Pr(IV), 2.54 MB (*17*).

We can conclude that Pt and Pr are ordered in the perovskite cell, a fact which can be understood in terms of the relatively large difference in ionic radii, which is about 20% in oxidation state 4+ and octahedral coordination (c.f. Shannon and Prewitt ionic radii (*18*), $^{VI}Pt^{4+}$ = 0.68 Å, $^{VI}Pr^{4+}$ = 0.78 Å). It is also interesting that the perovskite structure in this case forces Pr to be tetravalent, whereas very often both Pr(III) and Pr(IV) are present in nonstoichiometric and mixed-valence oxides, such as Pr_6O_{11} and $Ba_2PrCu_3O_{7-y}$ (*11*).

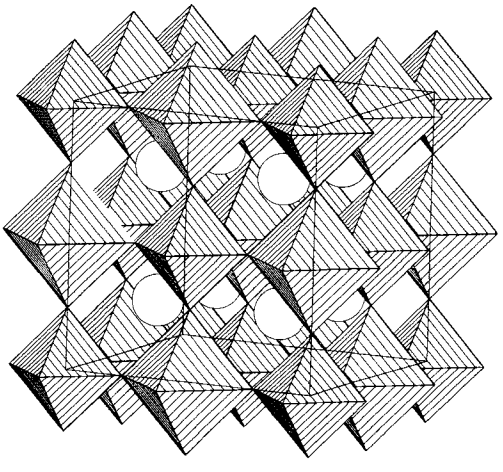

FIG. 6. Schematic representation of the Ba_2PtPrO_6 structure. The small octahedra represent the coordination polyhedra of Pt(IV) while the larger ones correspond to Pr(IV) ions in accordance with ionic radii.

TABLE II

BOND LENGTHS IN Ba_2PtPrO_6

Ba–O	2.966(6) × 12
Pt–O	2.049(3) × 6
Pr–O	2.146(3) × 6

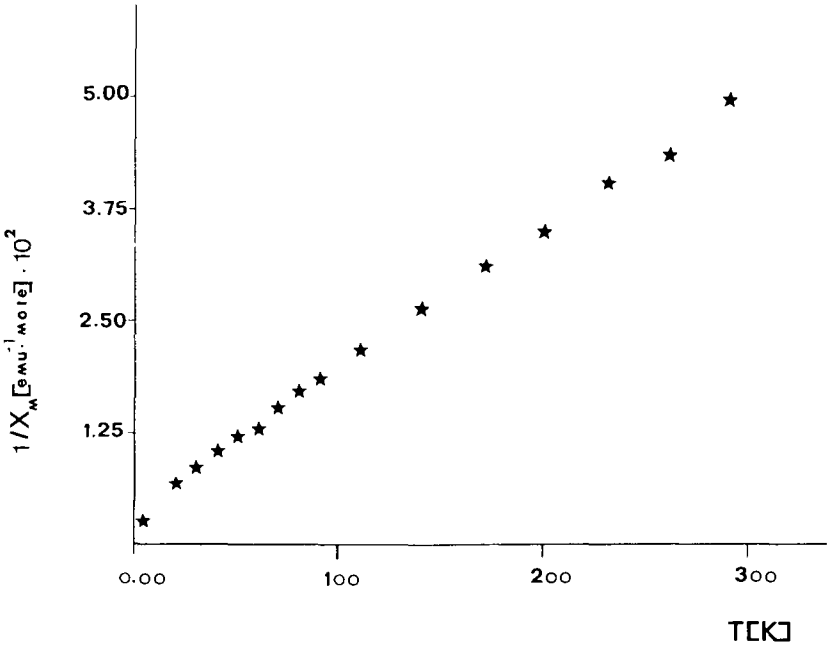

FIG. 7. Reciprocal molar magnetic susceptibility vs. temperature for the title compound. A Curie–Weiss behavior has been found.

Acknowledgments

One of us (C. J. D. H.) thanks the Dirección General de Investigación Científica y Técnica (M. E. C.) for a sabbatical grant. We also thank CICYT (grant MAT 89/0768), the Domingo Martínez Foundation, and E.I.T.E. for financial support.

References

1. F. S. GALASSO, "Structure, Properties and Preparation of Perovskite-Type Compounds," Pergamon Press, London (1970).
2. J. B. GOODENOUGH, *Prog. Solid State Chem.* **5,** 313 (1971).
3. J. B. GOODENOUGH AND J. M. LONGO, "Lundolt–Börnstein Numerical Tables. New Series," Vol. 4, Chap. 3, Springer-Verlag, Berlin (1970).
4. O. MÜLLER AND R. ROY, "The Major Ternary Structural Families," Springer-Verlag, Berlin (1974).
5. S. GELLER AND V. B. BALA, *Acta Crystallogr.* **9,** 1019 (1956).
6. M. MAREZIO, J. REMEIKA, AND P. DERNIER, *Acta Crystallogr. Sect. B: Struct. Crystallogr. Cryst. Chem.* **B26,** 2008 (1970).
7. A. J. SMITH AND A. J. WELCH, *Acta Crystallogr.* **13,** 653 (1960).
8. A. VEGAS, M. VALLET-REGI, J. GONZALEZ-CALBET, AND M. ALARIO-FRANCO, *Acta Crystallogr. Sect. B: Struct. Sci.* **B42,** 167 (1986).
9. G. DEMAZEAU, B. BUFFAT, M. POUCHARD, AND P. HAGENMULLER, *J. Solid State Chem.* **45,** 88 (1982).
10. Z. C. KANG, C. CARRANONI, I. SINY, G. NIHOUL, AND C. BOULESTEIX, *J. Solid State Chem.* **87,** 308 (1990).
11. E. MORÁN, U. AMADOR, M. BARAHONA, M. ALARIO-FRANCO, A. VEGAS, AND J. RODRIGUEZ-CARVAJAL, *Solid State Commun.* **67**(4), 369 (1988).
12. H. MÜLLER-BUSCHBAUM, *Angew. Chem. Int. Ed. Engl.* **28,** 1472 (1989).
13. H. M. RIETVELD, *J. Appl. Crystallogr.* **2,** 65 (1969).

14. D. B. WHILES AND R. A. YOUNG, *J. Appl. Crystallogr.* **14,** 149 (1981).

15. U. AMADOR, C. J. D. HETHERINGTON, E. MORÁN AND M. A. ALARIO-FRANCO, to be published.

16. I. B. BROWN AND ALTERMATT, *"Acta Crystallogr. Sect. B: Struct. Sci.* **B41,** 244 (1985).

17. A. MORRISH, "The Physical Principles of Magnetism," R. E. Krieger Publisher, N.Y. (1980).

18. R. D. SHANNON AND C. PREWITT, *"Acta Crystallogr. Sect. B: Struct. Crystallogr. Cryst. Chem.* **B25,** 925 (1969).